Annales Societatis Geologorum Poloniae (2013), vol. 83: 229–242.

NEEDLE-FIBRE CALCITE AND NANOFIBRES AS COMPONENTS OF HOLOCENE FISSURE-FILLING CARBONATES IN SOUTHERN POLAND

Michał GRADZIŃSKI, Renata JACH & Edyta GÓRNIKIEWICZ

Institute of Geological Sciences, Jagiellonian University, Oleandry 2a, 30-063 Kraków, Poland;
e-mails: michal.gradzinski@uj.edu.pl, renata.jach@uj.edu.pl, edytag89@gmail.com

Gradziński, M., Jach, R. & Górnikiewicz, E., 2013. Needle-fibre calcite and nanofibres as components of Holocene fissure-filling carbonates in southern Poland. *Annales Societatis Geologorum Poloniae*, 83: 229–242.

Abstract: The article deals with the carbonates, filling fissures in limestone bedrock and presently exposed in a south-facing rock wall of Kramnica hill (Pieniny Klippen Belt, southern Poland). The carbonates are composed of (i) needle-fibre calcite crystals, (ii) carbonate nanofibres, (iii) carbonate nanoparticles, and (iv) micrite and sparite calcite crystals. Detrital grains from the carbonate bedrock occur subordinately. The spatial relationships of the components give documentation that the nanofibres were formed simultaneously with or slightly later than the needle-fibre calcite crystals. There exists a continuous chain of forms from nanoparticles to elongated nanofibres. This, in turn, indicates that all the above morphological forms are related genetically. In relatively wide fissures, the carbonates studied formed stepped microterracettes, similar to those of speleothems, mainly of moonmilk type. Conversely, narrow fissures are completely filled with carbonates, which display parallel lamination. The carbonates were formed in the late Holocene. However, "dead carbon effect" precludes the possibility of any precise dating of them. Their $\delta^{13}C$ and $\delta^{18}O$ values are in ranges from -5.1‰ to -3.8‰ and from -6‰ to -4.7‰, respectively. The carbonates studied bear a strong resemblance to soil and spelean, moonmilk-type carbonates. This indicates that continuity exists between the depositional environments of soil and spelean carbonate.

Key words: speleothems, caliche, stable isotopes, radiocarbon dating, Pieniny Klippen Belt, Western Carpathians.

Manuscript received 25 November 2013, accepted 23 December 2013

INTRODUCTION

Needle-fibre calcite is a ubiquitous component of various continental carbonates. It was first recognized in soils and the underlying weathered carbonate bedrock in Poland (Iwanoff, 1905–1906). Morozewicz (1907, 1911) coined the term "lublinite" for such elongated carbonate crystals, with reference to the name of the city of Lublin, eastern Poland. However, further studies revealed that it is not an independent mineral phase, but rather represents a specific habit of low-magnesium calcite (Thugutt, 1929; Stoops, 1976; Bernasconi, 1981; see also Jones and Kahle, 1993 for discussion). Although needle-fibre calcite was at first described in a temperate-climate area, it attracted close attention as a common component of modern calcretes, developed in arid or semi-arid regions (James, 1972; Phillips and Self, 1987; Jones and Ng, 1988; Verrecchia, 1990; Alonso-Zarza, 2003; Alonso-Zarza and Jones, 2007; Wright, 2007; Zhou and Chafetz, 2009; Alonso-Zarza and Wright, 2010). Moreover, it occurs in fossil calcretes of various ages (Wright, 1984, 1986; Wright *et al.*, 1995; Kabanov *et al.*, 2010). The common occurrence of needle-fibre calcite in the soil environment of a temperate climate was fully confirmed at many sites in Europe (e.g., Kowalinski *et al.*, 1972; Strong *et al.*, 1992; Becze-Deák *et al.*, 1997; Loisy *et al.*, 1999; Łącka *et al.*, 2009; Barta, 2011; Millière *et al.*, 2011a, b). It was also detected in the soils of tropical Africa and Asia (e.g., Cailleau *et al.*, 2005; Owliaie, 2013). Besides its occurrence in soils, needle-fibre calcite is known also from caves. It is an important component of some speleothems almost all around the world. It was documented mostly in moonmilk-type deposits (e.g., Gradziński and Radomski, 1957; Stoops, 1976; Bernasconi, 1981; Gradziński *et al.*, 1997; Borsato *et al.*, 2000; Northup and Lavoie, 2001; Cañaveras *et al.*, 2006; Richter *et al.*, 2008; Curry *et al.*, 2009; Jones, 2010), but also in cave pisoids (cave pearls; Jones, 2009; Gradziński *et al.*, 2012a). Thus, the most common modes of occurrence for needle-fibre calcite are in the weathering zone and in caves located some metres below it.

However, information about needle-fibre calcite within shallow parts of its host rocks is scarce. In arid climatic conditions, this kind of calcite acts also as cement in young, porous carbonates (e.g., Supko, 1973; Ward, 1973; Sherman *et al.*, 1999). Dullo and Tietz (1984) analyzed the differentiation of the calcite, forming coatings within fissures in Steiermark, Austria. They noted the presence of needle-fibre

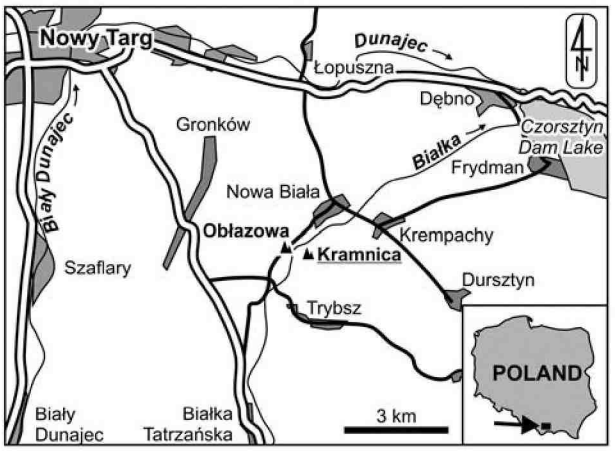

Fig. 1. Location of Kramnica hill

calcite of various habits. Some papers, published at the beginning of the 20th century, probably also described needle-fibre calcite from fissures, but there is no clear statement of whether the material analyzed was collected from soils and the weathering zone or from below them (e.g., Iwanoff, 1905–1906).

The study of needle-fibre calcite, using a scanning electron microscope (SEM), allows recognition of its considerable morphological variation (Dullo and Tietz, 1984; Jones and Ng, 1988; Jones and Kahle, 1993; Verrecchia and Verrecchia, 1994; Bajnóczi and Kovács-Kis, 2006; Cailleau, 2009a). This also showed that needle-fibre calcite is commonly associated with smaller carbonate fibres, variously termed micro-rods, needles and nanofibres (e.g., Philips and Self, 1987; Gradziński *et al.*, 1997; Borsato *et al.*, 2000; Zhou and Chafetz, 2009; Bindschedler *et al.*, 2010, 2012). Nanofibres, which are analogous in shape, can be also composed of organic matter (Bindschedler *et al.*, 2010).

Needle-fibre calcite grows typically in the vadose zone. Nonetheless, there are different opinions as to its origin. Several authors drew attention to the direct or indirect influence of micro-organisms, mainly fungi, on its formation (Wright, 1984, 1986; Olszta *et al.*, 2004; Cañaveras *et al.*, 2006; Blyth and Frisia, 2008; Richter *et al.*, 2008; Cailleau *et al.*, 2009a, b; Bindschedler *et al.*, 2010, 2012; Baskar *et al.*, 2011). Others regard needle-fibre calcite as a product of purely physico-chemical processes (Onac, 1995; Borsato *et al.*, 2000).

The present paper focuses on the specific occurrence of needle-fibre calcite crystals and nanofibres, which form the carbonate fillings of fissures in limestones below the weathering zone. It emphasizes the similarity of the above components to those known from soils and some spelean carbonates. On the basis of the example described, some measure of continuity between the depositional environments of soil and spelean carbonate is inferred.

ENVIRONMENTAL SETTING

Fissure-filling carbonates were found in a south-facing wall of a rocky hill, called Kramnica (50°04.140' 19°55.919'), in southern Poland (Figs 1, 2A). Kramnica is one of the twin hills forming a water gap in the Białka River, where it flows through the Pieniny Klippen Belt. The area has been protected as a nature reserve since 1959 (Grodzińska, 1979). The top of Kramnica is located at an altitude of 688 m, whereas the mean level of the Białka River is at an altitude of 630 m. The south-facing rock wall is about 30 m high. In the eastern part of the wall, there is an inclined shelf up to 2.5 m wide, which provides easy access to the central part of the wall, where the fissure-filling carbonates occur. At the foot of the rock wall, beneath the shelf, there is a small fan of rockfall material.

The hills forming the water gap are composed of a tectonized succession of mainly Jurassic rocks (Birkenmajer, 1979). Crinoidal and nodular limestones are exposed in rock cliffs. The south-facing wall of Kramnica is built of crinoidal limestone, which represents the Smolegowa Limestone Formation of Bajocian age (Birkenmajer, 1977). The limestone dips southward at an angle of 75°. The soil cover on the top of Kramnica is relatively thin. It consists of early-formed rendzina-like soils (Grodzińska, 1979).

The mean annual precipitation for the region ranges from 690–860 mm and the mean annual temperature varies from 5–5.5°C (Kostrakiewicz, 1982). However, differentiation of the microclimate is a typical characteristic of this region. Thus, higher mean annual temperatures reaching 8°C might be expected on the southern slopes (Kostrakiewicz, 1982). The Białka River water gap abounds in various vascular plants. The top of Kramnica is covered with a relict pine forest, whereas epilithic and xerothermic grass form isolated patches on the south-facing rock wall (Grodzińska, 1979).

MATERIAL AND METHODS

Carbonates were documented on the south-facing rock wall of Kramnica. The sampling of the carbonates was kept to an absolute minimum, because the area is under protection. The internal structures of the carbonates studied were observed under a standard petrographic optical microscope and a field emission SEM Hitachi S-4700, equipped with a NORAN Vantage energy dispersive spectrometer (EDS). SEM analyzes were performed, using a working distance of 15 mm, a 10 kV acceleration voltage, and a semi-conductor Si (Li) detector. The samples were mounted on SEM holders with silver glue and coated with C or Au. The mineral composition was analyzed by powder X-ray diffractometry (XRD), using a vertical XPert APD Philips goniometer (PW 1830).

The carbon and oxygen stable-isotope composition of eight samples was analysed at the Warsaw Isotope Laboratory for Dating and Environment Studies of the Polish Academy of Sciences. The calcite samples were dissolved in 100% phosphoric acid at 70°C, using a Kiel IV online carbonate preparation device, connected to a Thermo-Finnigan Delta Plus mass spectrometer. The quality of the analysis was controlled by NBS-19 international standard measurements. The $\delta^{13}C$ and $\delta^{18}O$ values are presented relative to the V-PDB. Analytical reproducibility was verified on the basis of the repeatability of the NBS-19 results, with an ob-

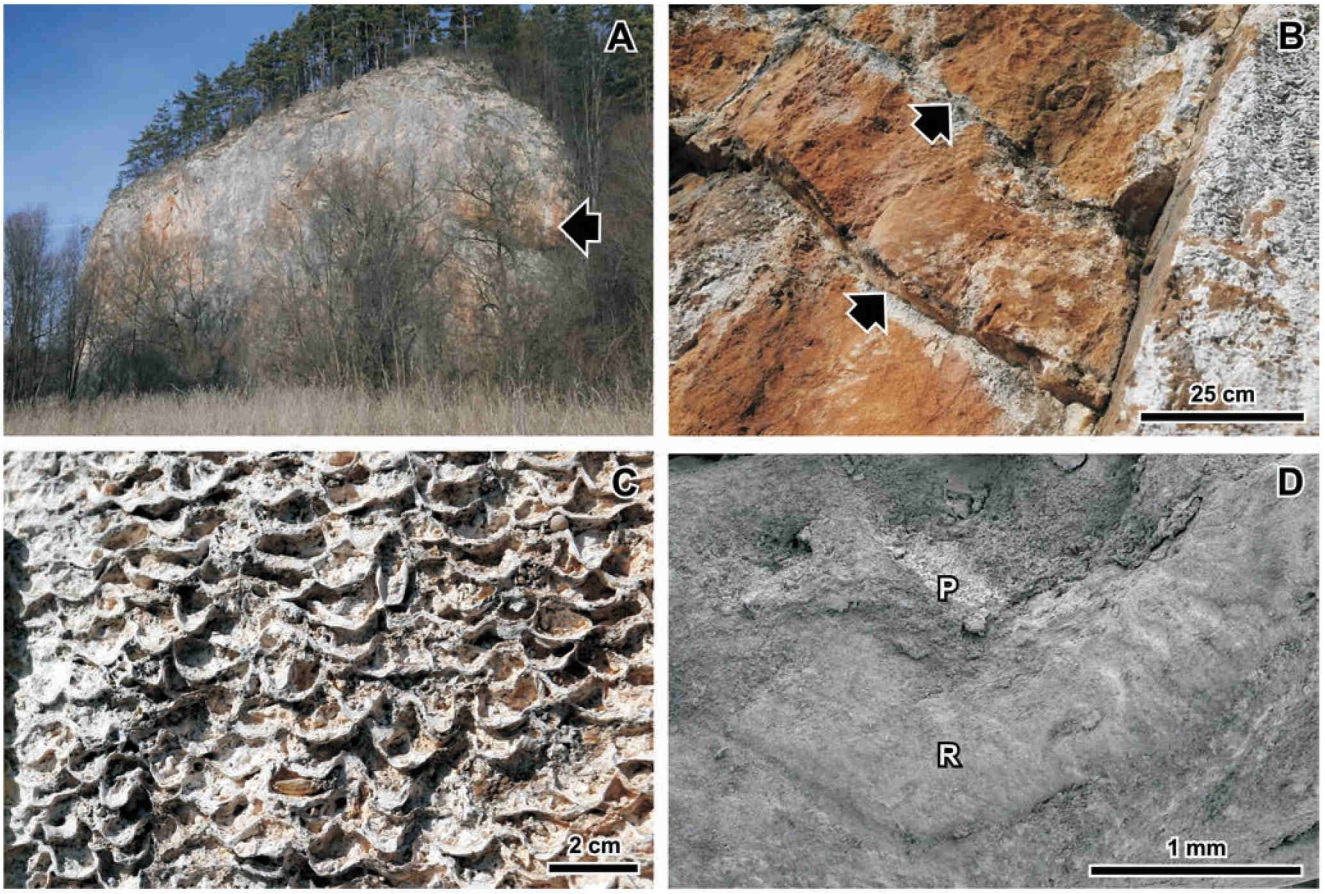

Fig. 2. Outcrop of fissure-filling carbonates. **A.** South-facing rock wall of Kramnica, whitish patches denote the position of carbonates studied, arrow indicates sampling area. **B.** Carbonates filling fissures (arrows) and exposed on the rock wall (right hand side of photo). **C.** Microterracettes covering the rock wall. **D.** SEM image of a microterracette; the lining microrim (R) is smooth, whereas the micropool (P) is relatively rough

served deviation of less than 0.07‰ for $\delta^{13}C$ and less than 0.12‰ for ^{18}O measurements.

One sample of carbonates was dated by the radiocarbon method at the Laboratory of Absolute Dating (Skała, Poland). Carbon dioxide, obtained by acid treatment, was converted to benzene. Measurements of radiocarbon concentration were carried out, using the scintillation technique by means of a new generation of low-background liquid scintillation counters, the HIDEX 300 SL (Krąpiec and Walanus, 2011). The radiocarbon date obtained was calibrated, using the OxCal program (Bronk Ramsey, 2009) and IntCal13 calibration data (Reimer *et al.*, 2013).

RESULTS

Field occurrence and internal structure

The carbonates are white to very light grey in colour; only occasionally they are very pale pink, owing to a residuum weathered from the limestone. They are hard, but friable, and in some places powdery. The carbonates occur on the surface of the rock wall and within the fissures cutting it (Fig. 2B). In the former case, they form patches exclusively in places where larger slabs of limestone had been displaced, which had resulted in the opening of fissures and exposure of the fissure-filling deposits (Fig. 2A). Thus, the carbonates grew in the fissures and subsequently were exposed at the surface. The patches are vertically elongated; they reach around 3 m in height and 0.5 m in lateral extent. The carbonates reach a thickness of 1.5 cm. The same carbonate material fills fissures, sections of which are visible in the rock wall (Fig. 2B). Fissures with openings reaching a few millimetres now are filled completely with carbonates.

On the rock wall, carbonates form stepped, overhanging microterracettes, composed of crests in the form of microims, which line micropools located behind them (Fig. 2C). The microrims dip outward in such a manner that their lowermost points are at their outermost parts. The microrims are smooth, whereas the micropools have a rougher relief, which is visible also under SEM (Fig. 2D).

The vertical distance between neighbouring microterracettes ranges from 3 to 13 mm. There is a clear tendency for the microteracettes to change shape with changes in the inclination of the underlying rock wall (Fig. 3A). The microterracettes covering the vertical wall are laterally more extensive, whereas the vertical distance between neighbouring microterracettes is relatively small (Fig. 3B). The horizontal dimension of the microterracettes decreases with increasing angle of the substrate. Accordingly, when the inclination of the rock wall changes to the point of overhanging, the mi-

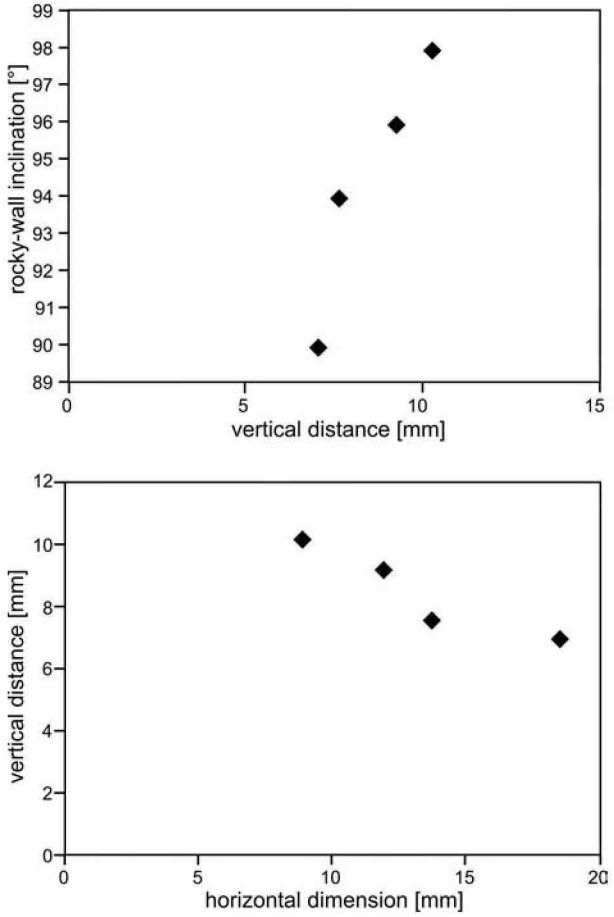

Fig. 3. Relationships between rock-wall inclination, vertical distance between microterracettes and their horizontal dimension; each point is mean of 10 measurements. **A.** Rock-wall inclination *versus* vertical distance of microterracettes. **B.** Vertical distance of microterracettes *versus* their horizontal dimension

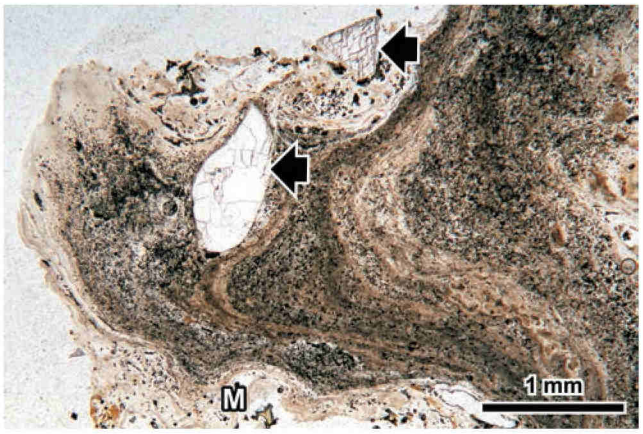

Fig. 4. Vertical cross section through a microterracette; arrows indicate trapped detrital grains, composed of Jurassic bedrock limestone, M – microstalactite, thin section, plane polarized light

croterracettes are shorter, their rims are more curved and the pools are narrower.

The carbonates studied display lamination, visible as a result of changes in porosity. Opaque laminae are more compact and made up of tightly packed components. The

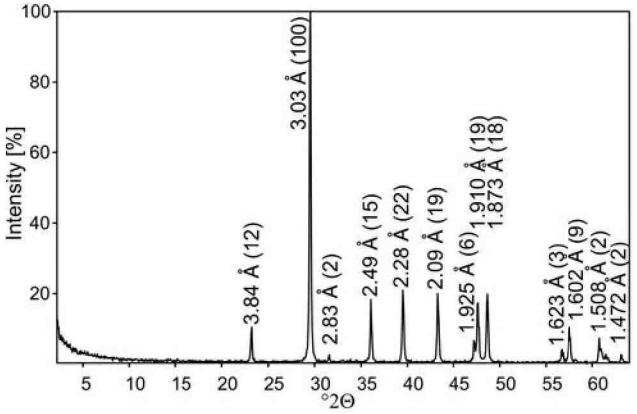

Fig. 5. XRD pattern of the fissure-filling carbonate. All peaks are related to calcite, and labelled with d_{hkl} value and relative intensity in %

intervening translucent laminae are more porous and formed by loosely packed components. The carbonates sealing the fissures are characterized by lamination that is roughly parallel to the fissure walls. Conversely, the laminae forming the microterracettes are curved and mimic the external relief (Fig. 4). The thickness of some laminae is greater in the lower parts of the microterracettes, with small microstalactites developed there.

Components

The carbonates are composed of the following components: (i) needle-fibre calcite crystals, (ii) calcite nanofibres, (iii) nanoparticles, and (iv) micrite and sparite crystals, which occur exceptionally. On the basis of the EDS results, all of the above components are interpreted as being composed of calcium carbonate with subordinate Mg content. XRD analyses detected calcite as the only autochthonous carbonate phase (Fig. 5). In addition to the above listed components, the carbonates studied comprise some carbonate grains, derived from the host rock, and small clumps of siliciclastic material (Fig. 4). The latter are probably a weathered residuum.

Needle-fibre calcite crystals

Needle-fibre calcite crystals are the most common component of the carbonates studied (Figs 6, 7, 8A, B, H). They represent two types of morphology: (i) composite fibrous crystals, which are the most common type, and (ii) polycrystalline chains.

The length of composite fibrous crystals varies from 2 μm to >100 μm, whereas their width falls within the range 0.4 μm to 2 μm. Such crystals are straight and are formed by four juxtaposed single fibrous crystals (Fig. 6D–F). They correspond to 4-lobed fibre crystals and paired rods (MA3 and MA4), distinguished by Jones and Kahle (1993) and Verrecchia and Verrecchia (1994), respectively. The juxtaposed fibrous crystals between 0.2 μm and 0.5 μm across are aligned along their long axes. The composite fibrous crystals display X-shaped or dumbbell-shaped cross-sections. The juxtaposed fibrous crystals seem to have primarily round

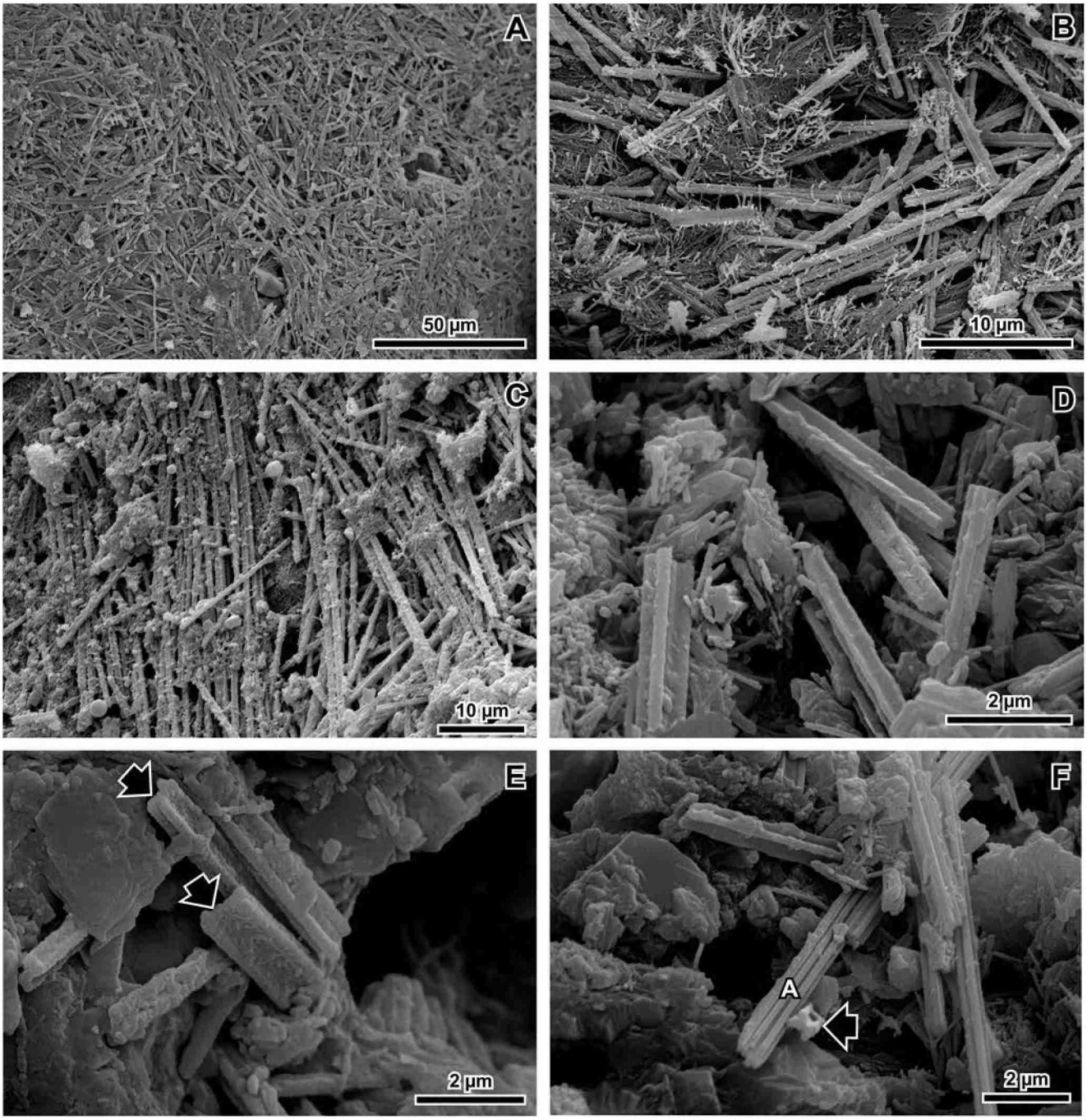

Fig. 6. Internal structure of fissure-filling carbonates; SEM images. **A.** Densely packed needle-fibre calcite crystals. **B.** Randomly oriented needle-fibre calcite crystals, associated with nanofibres. **C.** Parallel oriented needle-fibre calcite crystals. **D**. Needle-fibre calcite crystals of composite fibrous type. **E.** Needle-fibre calcite crystals of composite fibrous type, arrows indicate their dumbbell-shaped cross-section. **F.** Agglomerate composed of several straight fibrous crystals (A) and needle-fibre calcite crystals of composite fibrous type, arrow indicates their X-shaped cross-section

or exceptionally hexagonal cross-sections and smooth faces. Many of them are covered with nanofibres, nanoparticles or minute calcite crystals, which partly or completely obliterate the primary shape. Only in one sample studied, agglomerates of several straight fibrous crystals were found (Fig. 6F). The agglomerates are circular in cross-section and reach 1.5 µm across. They are akin to the crystals illustrated by Cailleau *et al.*. (2009b, figs 3.2, 9.2).

The composite fibrous crystals show rare imperfections, similar to those recognized by Bindschedler *et al.*. (2012). Between the majority of crystals, which display blunt terminations, some crystals with acute, irregular terminations occur (Fig. 7A). Other crystals are turned at an angle of between 140° and 160° (Fig. 7B) or slightly twisted along their long axes (Fig. 7C). Branching of some composite fibrous crystals was also noted (Fig. 7D).

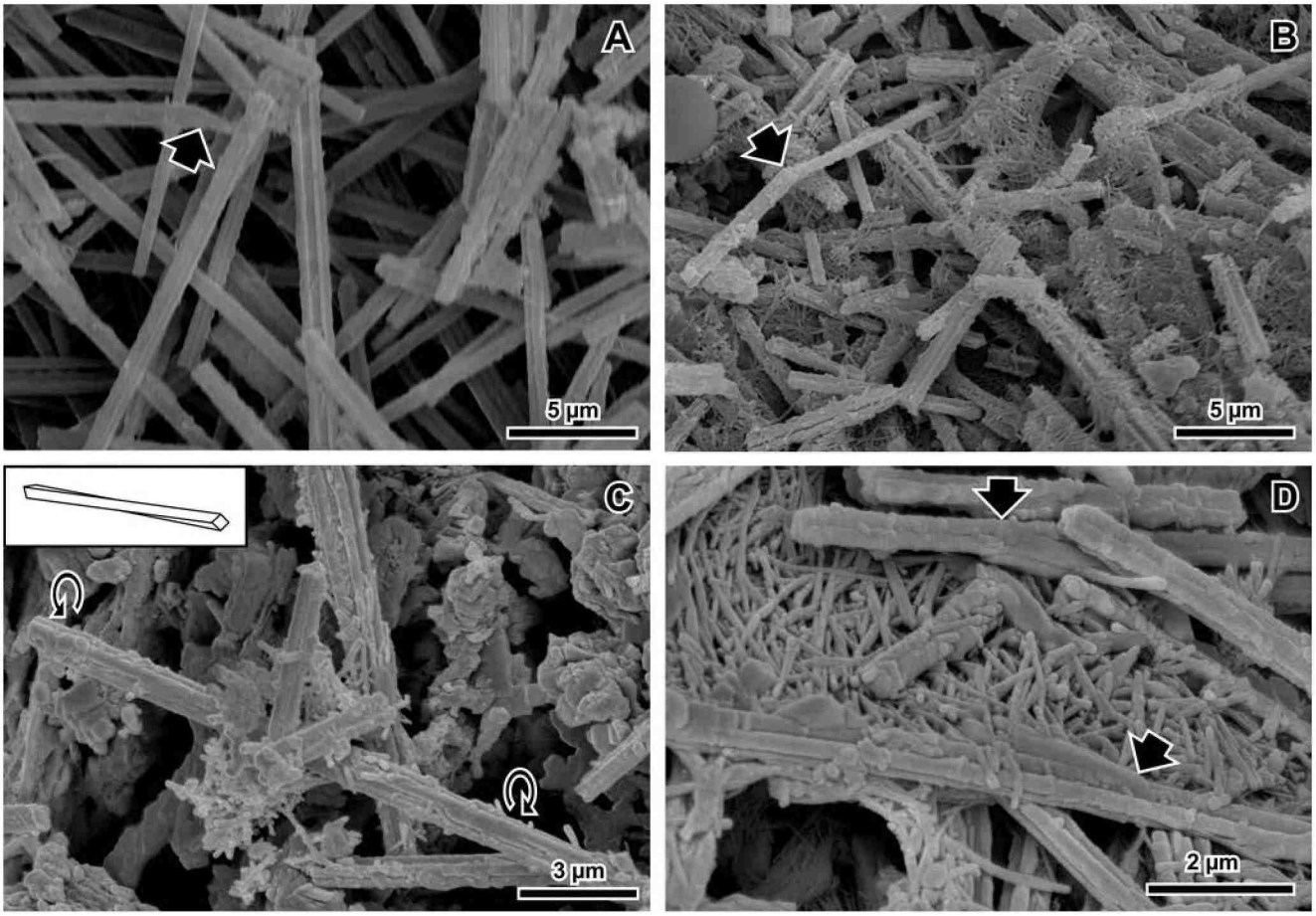

Fig. 7. Imperfections in needle-fibre calcite crystals; SEM images. **A.** Crystal with acute, irregular termination (arrow). **B.** Turned crystal associated with nanofibres, insert presents as an example a solid twisted in the same manner. **C.** Crystal twisted (arrows) along its long axis. **D.** Branching crystals (arrows) associated with dense mat of nanofibres

Needle-fibre calcite crystals are randomly or parallel distributed (Fig. 6A–C). The former pattern is definitely the more common. However, even in these cases there are some domains, in which the neighbouring crystals display a parallel or subparallel orientation. The parallel distributed needle-fibre crystals are tightly packed, whereas the randomly distributed ones show various types of packing, ranging from loose to tight.

Nanofibres

The nanofibres are curved and curled; they are 0.1–0.2 µm across (Figs 6B, 7B, D, 8A, B, G). Their diameters, with some rare exceptions, apparently have the same order of magnitude. Their lengths vary between 0.8 µm and >20 µm; it is impossible to ascertain the upper limit. Uncommonly, some of the nanofibres have bulbous terminations. The nanofibre surface appears to be smooth; an overgrowth of younger calcite crystals is exceptional. EDS examination suggests that nanofibres are composed of calcium carbonate. However, bearing in mind their minute sizes, this cannot be confirmed with certainty.

As a rule, the nanofibres form (i) clumps or (ii) a three-dimensional, pierced structure. Each clump contains several, curved nanofibres, which are woven and intertwined (Fig. 8B). They are closely packed, forming a dense mat with a fitted fabric. The pierced structures are composed of loosely arranged nanofibres, which are randomly distributed or arranged subparallel (Fig. 8A). The contact between neighbouring nanofibres is concavo-convex.

The nanofibres co-occur with the needle-fibre calcite crystals (Figs 6B, 7D, 8A, B). They stretch between neighbouring needle-fibre calcite crystals or cover them, which can result in the complete obliteration of their relief.

Fig. 8. Nanofibres and nanoparticles; SEM images. **A.** Loosely arranged nanofibres associated with needle-fibre crystal of composite fibrous type. **B.** Dense mat of nanofibres co-occurring with and covering a needle-fibre crystal of composite fibrous type. **C.** clump composed of nanoparticles with various shapes. **D.** Spherical, ellipsoidal, and rod-shaped nanoparticles. **E.** Clumps composed of spherical and ellipsoidal nanoparticles, associated with irregular micrite crystal (arrow). **F, G.** Rod-shaped nanoparticles and nanofibres. **H.** Nanoparticles covering a needle-fibre calcite crystal

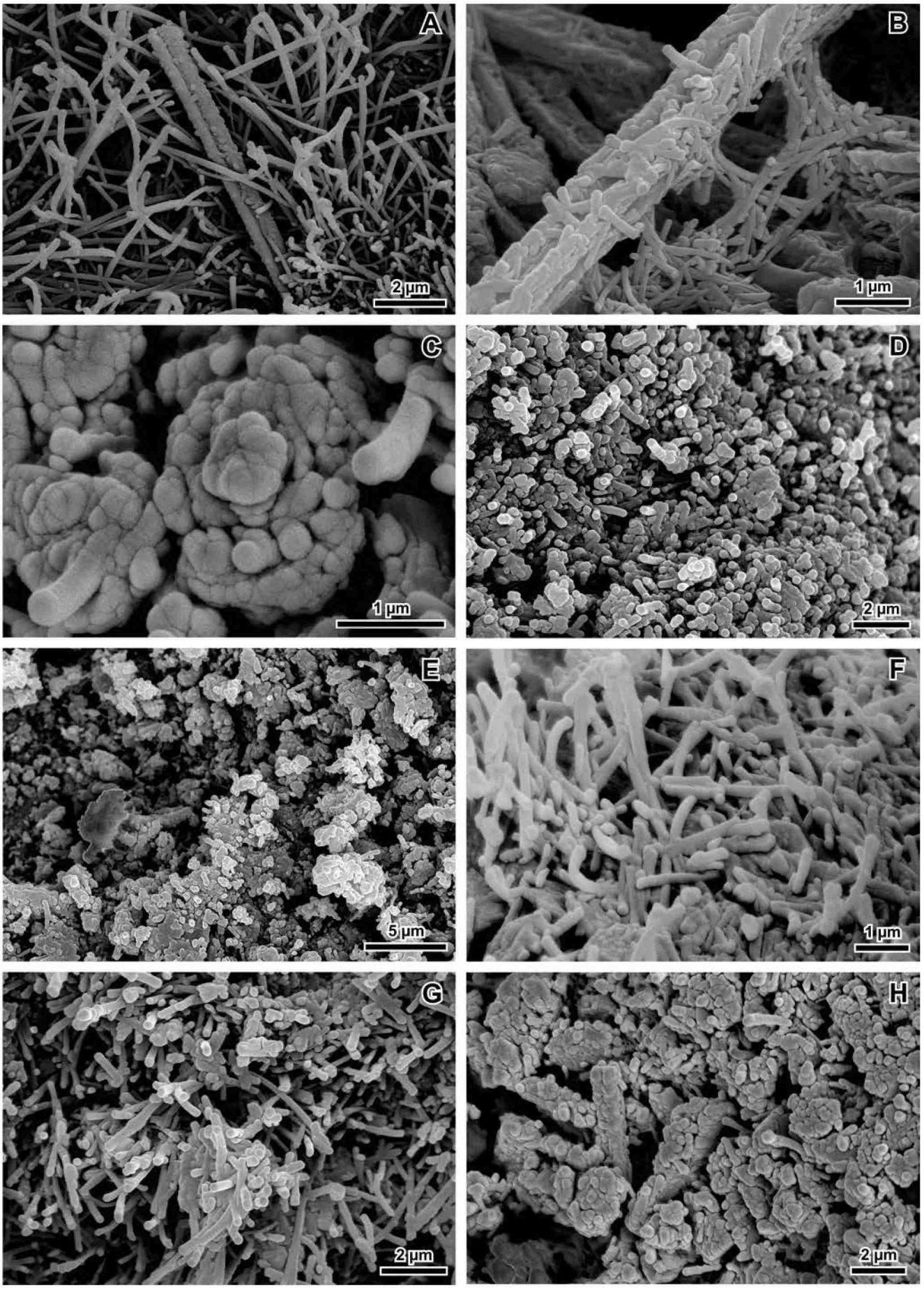
A
2 µm
B
1 µm
C
1 µm
D
2 µm
E
5 µm
F
1 µm
G
2 µm
H
2 µm

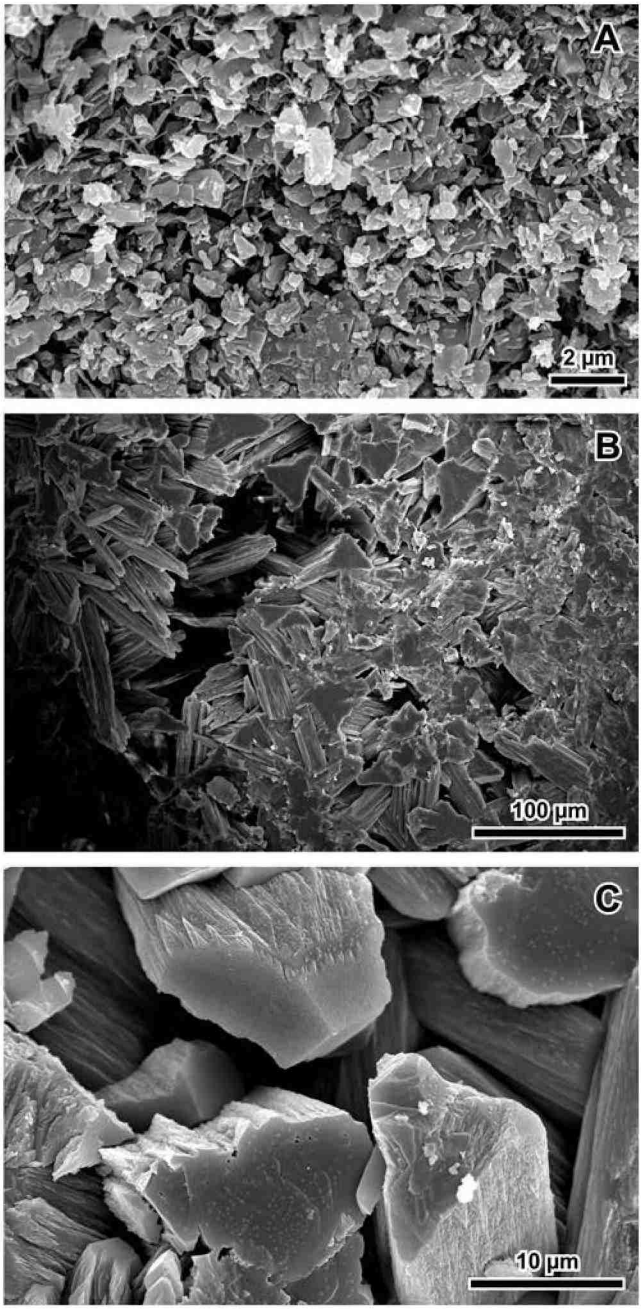

Fig. 9. Calcite crystals; SEM images. **A.** Irregular micrite crystals. **B.** Trigonal prisms with flat terminations, acicular subcrystals are visible. **C.** Trigonal prisms with acute terminations, acicular subcrystals are visible

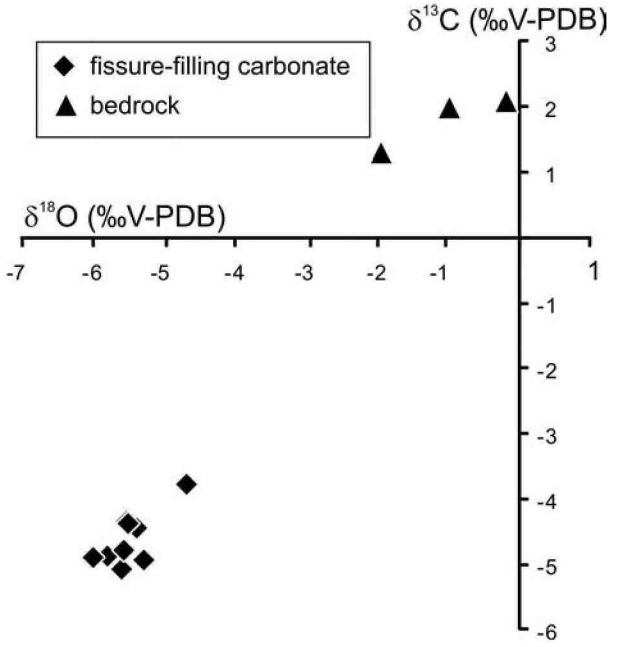

Fig. 10. Stable isotopic composition of fissure-filling carbonates and Jurassic limestone bedrock

Nanoparticles

Particles less than 1 µm across are named nanoparticles, following the terminology of Jones and Peng (2012). The majority of them are between 0.1 µm and 0.2 µm across (Fig. 8C–H). Such particles display various shapes: flat spheres, spheres, ellipsoids, and short rods. Several tightly packed nanoparticles form irregular clumps up to 15 µm across (Fig. 8E). The nanoparticles in one clump have different shapes and sizes (Fig. 8C). The nanoparticles are also spatially associated with nanofibres or cover the surface of the needle-fibre calcite crystals (Fig. 8G, H). Like the nanofibres, the nanoparticles most probably are composed of calcium carbonate, as inferred from EDS examination.

Micrite and sparite crystals

Irregular, plate-shaped crystals of micrite, up to 10 µm across, occur within the other components (Figs 8E, 9A). Their faces are poorly developed. Such crystals comprise needle-fibre calcite crystals and in particular, nanofibres or nanoparticles fused together.

Sparite crystals with incomplete faces represent another component (Fig. 9B, C). They have a habit of trigonal prisms with flat or acute terminations and elongated, spiky subcrystals visible on incomplete side faces. The sparite crystals are up to 100 µm in length. They line and in some cases fill completely the larger pores within the carbonates discussed.

Stable isotope composition

The stable isotope compositions of the bulk samples of carbonates studied are listed in Table 1 and presented in Fig. 10. The $\delta^{13}C$ and $\delta^{18}O$ values of the fissure-filling carbonates form a separate cluster. The $\delta^{13}C$ and $\delta^{18}O$ values fall within the range from -5.1‰ to -3.8‰ and from -6‰ to -4.7‰, respectively.

Radiocarbon dating

One sample of carbonates was dated. The conventional age of the carbonates is 4740 ± 110 years BP. The calibrated age is presented in Table 2. However, the age of the carbonates studied cannot be determined precisely. The radiocarbon age obtained most probably was modified by the so-called "reservoir effect" ("dead-carbon effect"), which results from the incorporation of inactive carbon from the

Table 1

Stable isotope composition of the carbonates studied (bulk samples)

Sample	$\delta^{18}O$	$\delta^{13}C$
KR1_1	-5.5	-4.3
KR1_2	-4.7	-3.8
KR1_3	-5.4	-4.4
KR3_1	-5.6	-5.1
KR3_2	-5.3	-4.9
KR4_1	-5.8	-4.9
KR5_1	-6.0	-4.9
KR11_1	-5.6	-4.8
KR11_2	-5.5	-4.4
KR1_4 *	-2.0	1.3
KR1_4 *	-0.2	2.1
KR1_4 *	-1.0	2.0

* Jurassic bedrock limestone

Table 2

Radiocarbon dating results

Sample	Laboratory number	Radiocarbon age [yr BP]	68.2% conf. interval		95.4% conf. interval	
			Cal. age range [yr BP]	Prob. [%]	Cal. age range [yr BP]	Prob. [%]
H3.4	MKL-1824	4740±110	3638–3496 3460–3376	43.9 24.3	3775–3326 3231–3174 3161–3119	91.8 2.0 1.6

bedrock into the growing carbonates (e.g., Pazdur *et al.*, 1988 and references therein). This effect also was confirmed from moonmilk speleothems in the Italian Alps, which were composed of needle-fibre calcite crystals and nanofibres (Borsato *et al.*, 2000) in a similar manner to the carbonates studied. In those speleothems, the so-called "apparent age", that is the difference between the true age and the conventional age, equalled ~1.1 ka and ~3 ka. Thus, it may be accepted only that the carbonates studied were formed between about 3500 cal years BP and 1950.

DISCUSSION

Relationship between components

The main components of the carbonates studied are needle-fibre calcite crystals and nanofibres. Such an association, composed of analogous components, commonly occurs in soils and speleothems (Jones and Ng, 1988; Loisy *et al.*, 1999; Richter *et al.*, 2008; Cailleau *et al.*, 2009a; Bindschedler *et al.*, 2010, 2012). Some authors postulated a genetic relationship between these two components, whereas others suggest that they owe their origins to different processes. The example described does not shed light on whether there really exists a genetic relationship between these two components; it simply confirms their co-occurrence in the vadose zone. Nonetheless, the spatial relationship between the nanofibres and the needle-fibre calcite crystals indicates that the former are not older than the latter (Figs 6B, 8A, B). Both components could have originated simultaneously or the nanofibres can slightly postdate the needle-fibre calcite crystals. Moreover, the shape and spatial arrangements of the nanofibres confirm the previous opinions of Borsato *et al.* (2000), Cailleau *et al.* (2009a) and Bindschedler *et al.* (2010) that the nanofibres or their precursors, if any, must have behaved in a plastic manner.

Forms that were similar in shape and size to the nano-particles described here were reported by Zhou and Chafetz (2009) from Texas caliche and by Jones and Peng (2012) from hot-spring deposits in China. Analogues nanoparticles also were produced experimentally in laboratory conditions and interpreted as an amorphous phase of calcium carbonate (Bontognali *et al.*, 2008; Xu *et al.*, 2008). The occurrence of amorphous carbonate as a product of biomineralization processes was noted in the calcareous skeletons of many organisms (e.g., Addadi *et al.*, 2003). Such a phase is transformed relatively quickly into vaterite, aragonite or calcite (e.g., Rodriguez-Blanco *et al.*, 2011). Thus, it seems probable that the nanoparticles discussed were composed of amorphous calcium carbonate. It is impossible to state if they are still composed of an amorphous phase or represent a specific type of calcitic pseudomorph. The nanoparticles comprise only one component that is mixed with the others. Accordingly, the XRD analyses, indicating the presence of calcite, provide information only about a bulk sample.

It is interesting to note that the formation of the nano-particles described so far commonly results from either the presence of several additives in a parent solution, many of them organic components, or the activity of (micro-)organisms (Xu *et al.*, 2005; Bontognali *et al.*, 2008). Therefore, there is an implication that the nanoparticles described were formed under the direct or indirect influence of micro-organisms. This seems to be in line with the postulated organic effect in the formation of needle-fibre calcite crystals and nanofibres (e.g., Blyth and Frisia, 2008; Richter *et al.*, 2008; Cailleau 2009a, b; Bindschedler, 2010, 2012), which co-occur with the nanoparticles in the carbonates discussed.

Nanoparticles are associated with nanofibres in the samples studied (Fig. 8G). The analysis of their sizes and shapes adds a new dimension to the discussion of nanofibre origin. Nanoparticles display a wide spectrum of shapes, from tightly packed flattened spheres, showing significant compaction, to elongated rods (Fig. 8C–F). The rods are juxtaposed with nanofibres, which also is the case for recent caliche from Texas (Zhou and Chafetz, 2009). Both components share the same diameter, a circular cross-section and a smooth surface. Some rods have also bulbous terminations, similar to those of some nanofibres. All these facts lead to the conclusion that there is no clear-cut boundary between the two categories. In fact, they can represent a continuous chain of forms, which owe their origin to similar processes or even the same process. The solution-precursor-solid mechanisms experimentally confirmed by Olszta *et al.* (2004) and the influence of an organic template postulated by Bindschedler *et al.*. (2010, 2012) are plausible. The morphological variability of nanoparticles and nanofibres could

have resulted from other additional factors, such as, for instance, the amount and chemistry of the parent solution, space limitations or the geometry of the micro-environments. Accepting the above facts and the postulated amorphous origin of the nanoparticles, it may be hypothesized that the nanofibres were formed, or still are being formed from amorphous calcium carbonate (see also Cailleau *et al.*, 2009a).

Isotopic composition

There is a growing interest in needle-fibre calcite isotope compositions. Data on the stable isotope ratio of carbonates comprising calcite of this type have been reported from many localities (Bajnóczi and Kovács-Kis, 2006; Cailleau *et al.*, 2009a, b; Millière, 2011a, b). The stable isotope composition of the carbonates discussed falls within the same range as the composition of needle-fibre calcite from the soils of Reims and Burgundy, France (Cailleau *et al.*, 2009b), Benasque, Spain (Millière, 2011b). It is also similar to the composition of bulk samples of pedogenic carbonates and moonmilk speleothems. The former were studied from Várhegy, in Budapest, Hungary (Bajnóczi and Kovács-Kis, 2006), whereas the latter were from Tunnel Cave, Germany (Richter *et al.*, 2008).

A comparison between the $\delta^{13}C$ values of the carbonates studied and other Holocene carbonates from the region shows a similarity to some speleothems from the Tatra caves. The Holocene stalagmite SC2, crystallized in Szczelina Chochołowska cave, located 30 km to southwest of Kramnica at an altitude of 1050 m, can serve as an example (Gradziński *et al.*, 2009). However, these values are higher than those obtained for the recent tufa stromatolites, growing at a distance of about 20 km to the east, at an altitude of about 650 m (Szulc and Smyk, 1994).

The $\delta^{13}C$ values of the carbonates discussed are located slightly above the upper limit of this parameter for carbonates receiving water charged with soil CO_2, associated with C3 pathway plants (Baker *et al.*, 1997). This might indicate that: (i) intense degassing of CO_2 preceded the crystallization of the carbonates, (ii) relatively heavy atmospheric CO_2 contributed to the solution, (iii) carbonate molecules derived from limestone bedrock substantially contaminated the solution, (iv) small carbonate particles of limestone bedrock were introduced into the samples stu–died (Fig. 4), or (v) crystallization proceeded out of isotopic equilibrium. It is impossible to support unequivocally any of the above possibilities. However, the third one is indirectly supported by the dating result presented above.

It is possible to discuss the conditions of crystallization, using an equation formulated by O'Neil *et al.* (1969) and later modified by Friedman and O'Neil (1977):

$$10^3 \ln \alpha_{c-w} = 2.78(10^6 T^{-2}) - 2.89 \qquad (1)$$

where T is the temperature of crystallization (absolute scale) and α_{c-w} is the oxygen equilibrium fractionation factor between calcite and water according to the formula:

$$\alpha_{c-w} = \frac{1000 + \delta^{18}O_c}{1000 + \delta^{18}O_w} \qquad (2)$$

As the $\delta^{18}O$ of precipitation in the region is unknown, the values of $\delta^{18}O$ of spring fed by shallow-circulating water can be used as a proxy for the parental water. Rajchel *et al.* (2005) reported that the Bachledów Spring, located about 15 km from the study site, issues water with a mean $\delta^{18}O$ = -10.81‰ V-SMOW. Calculations show that the calcites studied should have grown in a temperature range of between -7.8°C and -3.3°C. Thus, these unacceptable results can be explained in the following ways: (i) $\delta^{18}O$ of the parental water was higher than the $\delta^{18}O$ of groundwater in the region, (ii) small carbonate particles of limestone-bedrock were introduced into the samples studied, or (iii) crystallization proceeded out of isotopic equilibrium. Although the carbonates studied contain some detrital admixtures, the autochthonous crystals definitely predominate and the second possibility can be ruled out. The third possibility may be attributed to the fast degassing of CO_2, which might be plausible. However, the weak correlation of $\delta^{18}O$ and $\delta^{13}C$ (r^2 = 0.56) does not strongly support such a scenario. Intense degassing is hardly expected in poorly ventilated fissures (see Gradziński *et al.*, 2012b). However, crystallization out of isotopic equilibrium can also result from microbial influence (Gradziński, 2003).

The calcite grew in the vadose zone, above the water table. Thus, a higher $\delta^{18}O$ of the parental water than that of the groundwater in the region can be explained in a twofold manner. The growing calcite may have been supplied with water precipitated only in the warm seasons, that is, water with a higher $\delta^{18}O$ than the annual weighted mean in the region. In the Tatras, at an altitude of 1100 m, the $\delta^{18}O$ of summer precipitation is around 3.5‰ higher than the annual weighted mean (Rozanski and Dulinski, 1988). The difference is slightly smaller in Kraków, at an altitude of 205 m, where it equals around 2.5‰ (Duliński *et al.*, 2001). Assuming the above values, the $\delta^{18}O$ of the parental water in the warm seasons may have equalled -7.31‰ V-SMOW and -8.31‰ V-SMOW in the study area. Application of these values in the calculations leads to temperature ranges of 4.9°C – 10.1°C and 1.0°C – 6.1°C, respectively. These values can be accepted, as they are close to the mean annual temperature in the region (Kostrakiewicz, 1982). Precipitation of the calcite studied in the warmer seasons seems to be in line with the conclusions reached by Millière *et al.*. (2011b), who demonstrated seasonal growth of needle-fibre calcite in the soils in Switzerland.

Another process that can result in higher values of the $\delta^{18}O$ of the parental water is evaporation, which preferentially removes light oxygen from the solution. On the one hand, evaporation can be expected to occur on the south-facing rock wall. However, on the other hand, this process should not be very efficient in fissures that are at least partly isolated. On the assumption that evaporation had an influence on the isotopic composition of the parental water and the growing calcites, the growth of the calcites in the warm seasons is indicated. Therefore, this leads to the conclusion that the calcites studied were formed mainly in the warmer seasons. This conclusion is closely analogous to the mode of origin, discussed in the preceding paragraph.

Conditions of growth

Microterracettes, similar to those found at Kramnica, are typical of carbonates formed from a thin film of flowing water in the conditions of the vadose zone. They are found in travertines (e.g., Julia, 1983; Pentecost, 2005; Hammer *et al.*, 2010) and speleothems, mainly those developed on overhanging walls (Hill and Forti, 1997). They are especially common in moonmilk speleothems, where their microrim is inclined downward, in a similar manner to those in the examples studied (Gradziński *et al.*, 2010). It is inferred that this shape results from the plastic consistency of fresh moonmilk, which allows it to creep down the cave wall (Gradziński and Radomski, 1957). In the case discussed, the development of microterracettes is probably limited to the wider fissures, which direct the film of water seeping into the vadose zone. This would explain their patchy occurrence. The water-soaked carbonates behaved in a plastic manner, as in the case of moonmilk speleothems. The narrow fissures probably were not occupied by seeping water, which resulted in the filling of them by carbonates without microterracette relief, instead displaying lamination parallel to the fissure walls.

Although similar microterracettes can originate, as a result of microbial stabilization of detrital grains flushed with percolating water (Gradziński *et al.*, 2010), this is not the case for the Kramnica carbonates. If the carbonate components were transported from the overlying weathering zone, fragmentation might be expected, accompanied by mixing with other non-carbonate components and limestone fragments, as a result of disintegration of the host rock. Conversely, only a subordinate amount of allochthonous detrital particles, derived from the weathering zone or the host limestones, contributed to the carbonates in question and the fine carbonate components do not show significant disintegration.

If each of the above discussed arguments is taken into account, it might be accepted that the carbonates studied grew within fissures in the limestone host-rock. They originated most probably under the direct or indirect influence of micro-organisms. Subsequently, some voids within the carbonates were filled with late sparry cements. The lack of any macro- or microstructures, connected to root systems, indicates that their formation took place without any direct contact with roots. The depth below the soil cover is hard to ascertain, since the former topography of Kramnica may have differed from the present one. Nonetheless, it is likely that the distance to the soil cover located at the top of Kramnica was more than 15 m. Some patches of the initial soils associated with rocky shelves and clumps of plants may have been located a smaller distance away. Therefore, in terms of their growth within a host rock, the carbonates discussed bear a strong resemblance to penetrative caliche (Rossinsky *et al.*, 1992) and fissure calcretes (endostromatolites) (Lauriol and Clark, 1999; Lacelle *et al.*, 2009). The carbonates described from Steiermark by Dullo and Tietz (1984) seem to be their closest recognized counterparts.

The fissure-filling carbonates described are the next example of continental carbonates, in which needle-fibre calcite and nanofibres are the basic components. The carbonates discussed are formed in a specific environment, located between the two described previously and the widely discussed ones, namely the weathering zone, including soil and caves. These environments so far have been regarded as two separate entities. Thus, the fissure-filing carbonates are a "missing link", which indicates that a genetic connection exists between pedogenic and spelean carbonate depositional environments.

CONCLUSIONS

1. The carbonates filling fissures in a south-facing rock wall of Kramnica hill are composed of needle-fibre calcite crystals, carbonate nanofibres, carbonate nanoparticles, and subordinately by micrite and sparite calcite crystals. Detrital grains from the carbonate bedrock occur as a minor admixture.

2. There exists a continuous chain of forms from flattened, spherical nanoparticles through rod-shaped ones to elongated nanofibres. This suggests that all of the above morphological forms are genetically related.

3. The nanoparticles and nanofibres could have been precipitated as amorphous carbonates. The nanofibres were formed simultaneously with or slightly later than the needle-fibre calcite crystals.

4. The carbonates studied are autochthonous components, which most probably owe their origin to an organic influence. They grew within fissures, cutting the carbonate bedrock. Their oxygen isotopic composition suggests they grew in the warm seasons, whereas their carbon isotopic composition documents the dominance of soil CO_2, connected with C3 plants in the carbonate system.

5. In relatively wide fissures, the carbonates studied formed stepped microterracettes and thus bear a strong resemblance to speleothems of moonmilk type. Conversely, narrow fissures are completely filled with carbonates, which display parallel lamination.

6. The carbonates discussed are related in origin to some soil and spelean carbonates. They were formed in fissures, that is, in a specific environment located between soils and caves. This indicates that a continuum exists between the carbonates deposited in these two environments, so far considered separately in terms of their modes of origin.

Acknowledgements

The authors are indebted to the Regional Directorate for Environmental Protection in Kraków for giving permission for the fieldwork. Thanks go also to Marek Duliński and Helena Hercman for stimulating discussion, to Anna Lewandowska for her help with XRD, as well as to Anna Łatkiewicz and Beata Zych for operating the SEM. The paper has greatly benefited from the reviews by Guillaume Cailleau and Tadeusz Peryt, and from editorial work by Bartosz Budzyń and Frank Simpson.

REFERENCES

Addadi, L., Raz, S. & Weiner, S., 2003. Taking advantage of disorder: amorphous calcium carbonate and its roles in biomineralization. *Advanced Materials*, 15: 959–970.

Alonzo-Zarza, A. M., 2003. Palaeoenvironmental significance of palustrine carbonates and calcretes in geological record. *Earth-Science Reviews*, 60: 261–298.

Alonso-Zarza, A. M. & Jones, B., 2007. Root calcrete formation on Quaternary karstic surfaces of Grand Cayman. *Geologica Acta*, 5: 77–88.

Alonso-Zarza, A. M. & Wright, V. P., 2010. Calcretes. In: Alonso-Zarza, A. M. & Tanner, L. H. (eds), *Carbonates in Continental Settings: Facies, Environments and Process. Developments in Sedimentology*, 61, pp. 225–267.

Bajnóczi, B. & Kovács-Kis, V., 2006. Origin of pedogenic needle-fiber calcite revealed by micromorphology and stable isotope composition – a case study of a Quaternary paleosol from Hungary. *Chemie der Erde*, 66: 203–212.

Baker, A., Ito, E., Smart, P. & McEwan, R., 1997. Elevated and variable values of ^{13}C in speleothems in a British cave system. *Chemical Geology*, 136: 263–270.

Barta, G., 2011. Secondary carbonates in loess-paleosoil sequences: A general review. *Central European Journal of Geosciences*, 3: 129–146.

Baskar, S., Baskar, R. & Routh, J., 2011. Biogenic evidences of moonmilk deposition in the Mawmluh Cave, Meghalaya, India. *Geomicrobiology Journal*, 28: 252–256.

Becze-Deák, J., Langohr, R. & Verrecchia, E. P., 1997. Small scale secondary $CaCO_3$ accumulations in selected sections of the European loess belt. Morphological forms and potential for paleoenvironmental reconstruction. *Geoderma*, 76: 221–252.

Bernasconi, R., 1981. Mondmilch (Moonmilk): Two questions of terminology. In: Beck, B. F. (ed.), *Eighth International Congress of Speleology, Proceedings, Volume 1*. National Speleological Society, Bowling Green, pp. 113–116.

Bindschedler, S., Millière, L., Cailleau, G., Job, D. & Verrecchia, E. P., 2010. Calcitic nannofibres in soils and caves: a putative fungal contribution to carbonatogenesis. In: Pedley, H. M. & Rogerson M. (eds), *Tufas and Speleothems. Unravelling the Microbial and Physical Controls*, *Geological Society Special Publication*, 336: 225–238.

Bindschedler, S., Millière, L., Cailleau, G., Job, D. & Verrecchia, E. P., 2012. An ultrastructural approach to analogies between fungal structures and needle fiber calcite. *Geomicrobiology Journal*, 29: 301–312.

Birkenmajer, K., 1977. Jurassic and Cretaceous lithostratigraphic units of the Pieniny Klippen Belt (Carpathians) in Poland. *Studia Geologica Polonica*, 45: 49–108.

Birkenmajer, K., 1979. *Przewodnik geologiczny po pienińskim pasie skałkowym*. Wydawnictwa Geologiczne, Warszawa, 237 pp. [In Polish].

Blyth, A. J. & Frisia, S., 2008. Molecular evidence for bacterial mediation of calcite formation in cold high-altitude caves. *Geomicrobiology Journal*, 25: 101–111.

Bontognali, T. R. R., Vesconcelos, C., Warthmann, R. J., Dupraz, C., Bernasconi, S. M. & McKenzie, J. A., 2008. Microbes produce nanobacteria-like structures, avoiding cell entombment. *Geology*, 36: 663–666.

Borsato, A., Frisia, S., Jones, B. & van der Borg, K., 2000. Calcite moonmilk: crystal morphology and environment of formation in caves in the Italian Alps. *Journal of Sedimentary Research*, 70: 1179–1190.

Bronk Ramsey, C., 2009. Bayesian analysis of radiocarbon dates. *Radiocarbon*, 51: 337–360.

Cailleau, G., Braissant, O., Dupraz, C., Aragno, M., & Verrecchia, E. P., 2005. Biologically induced accumulations of $CaCO_3$ in orthox soils of Biga, Ivory Coast. *Catena*, 59: 1–17.

Cailleau, G., Dadras, M., Abolhassani-Dadras S., Braissant O. & Verrecchia, E. P., 2009a. Evidence for an organic origin of pedogenic calcitic nanofibres. *Journal of Crystal Growth*, 311: 2490–2495.

Cailleau, G., Verrecchia, E. P., Braissant, O. & Emmanuel, L., 2009b. The biogenic origin of needle fibre calcite. *Sedimentology*, 56: 1858–1875.

Cañaveras, J. C., Cuezva, S., Sanchez-Moral, S., Lario, J., Laiz, L., Gonzalez, J. M. & Saiz-Jimenez, C., 2006. On the origin of fiber calcite crystals in moonmilk deposits. *Naturwissenschaften*, 93: 27–32.

Curry, M. D., Boston, P. J., Spilde, M. N., Baichtal, J. & Campbell, A. R., 2009. Cottonballs, a unique moonmilk, and abundant subaerial moonmilk in Cataract Cave, Tongass National Forest, Alaska. *International Journal of Speleology*, 38: 111–128.

Duliński, M., Florkowski, T., Grabczak, J. & Różański, K., 2001. Twenty-five years of systematic measurements of isotopic composition of precipitation in Poland. *Przegląd Geologiczny*, 49: 250–256. [In Polish, English summary].

Dullo, W-Ch. & Tietz, G. F., 1984. Kalzitische Whisker und Dendritenkristalle als Vorstufe zur Füllung von Klüften in Kalken. *Mitteilungen der Gesellschaft der Geologie-und Bergbaustudenten in Österreich*, 30/31: 217–234.

Friedman, I. & O'Neil, J. R. 1977. Compilation of stable isotope fractionation factors of geochemical interest. In: Fleischer, M. (ed.), *Data of Geochemistry. US Geological Survey Professional Paper*, 440–KK: 1–12.

Gradziński, M., 2003. Bacterial influence on speleothem oxygen isotope composition: An example based on cave pisoids from Perlová Cave (Slovakia). *Geologica Carpathica*, 54: 199–204.

Gradziński, M., Chmiel, M. J., Lewandowska, A. & Michalska-Kasperkiewicz, B., 2010. Siliciclastic microstromatolites in a sandstone cave: Role of trapping and binding of detrital particles in formation of cave deposits. *Annales Societatis Geologorum Poloniae*, 80: 303–314.

Gradziński, M., Chmiel, M. J. & Motyka, J., 2012a. Formation of calcite by chemolithoautotrophic bacteria – a new hypothesis, based on microcrystalline cave pisoids. *Annales Societatis Geologorum Poloniae*, 82: 361–369.

Gradziński, M., Duliński, M., Hercman, H., Górny, A. & Przybyszowski, S., 2012b. Peculiar calcite speleothems filling fissures in calcareous sandstones and their palaeohydrological and palaeoclimatic significance: an example from the Polish Carpathians. *Geological Quarterly*, 56: 711–732.

Gradziński, M., Hercman, H., Kicińska, D., Barczyk, G., Bella, P. & Holúbek, P., 2009. Karst in the Tatra Mountains – developments of knowledge in the last thirty years. *Przegląd Geologiczny*, 57: 674–684. [In Polish, English summary].

Gradziński, M., Szulc, J. & Smyk, B., 1997. Microbial agents of moonmilk calcification. In: Jeannin, P.-Y. (ed.), *Proceedings of the 12th International Congress of Speleology*, *Volume 1*. International Union of Speleology, Basel, pp. 275–278.

Gradziński, R. & Radomski, A., 1957. Cavern deposits of "rock milk" in the Szczelina Chochołowska Cave. *Rocznik Polskiego Towarzystwa Geologicznego*, 26: 63–90. [In Polish, English summary].

Grodzińska, K., 1979. Map of plant communities in the nature reserve of "Przełom Białki pod Krempachami" (Białka River Gorge at Krempachy, Pieniny Klippen Belt). *Ochrona Przyrody*, 42: 29–73. [In Polish, English summary].

Hammer, Ø., Dysthe, D. C. & Jamtveit, B., 2010. Travertine terracing: patterns and mechanisms. In: Pedley, H. M. & Rogerson, M. (eds), *Tufas and Speleothems: Unravelling the Microbial and Physical Controls. Geological Society Special*

Publications, 336: 345–355.

Hill, C. & Forti, P., 1997. *Cave Minerals of the World*. National Speleological Society, Huntsville, pp. 1–463.

Iwanoff, L. L., 1905–1906. Ein wasserhaltiges Calciumcarbonat aus den Umgebung von Nowo-Alexandria (Guv. Lublin). *Annuaire Géologique et Minéralogique de la Russie*, 8: 23–25. [In Russian, German summary].

James, N. P., 1972. Holocene and Pleistocene calcareous crust (caliche) profiles: Criteria for subaerial exposure. *Journal of Sedimentary Petrology*, 42: 817–836.

Jones, B., 2009. Cave pearls – the integrated product of abiotic and biotic processes. *Journal of Sedimentary Research*, 79: 689–710.

Jones, B., 2010. Microbes in caves: agents of calcite corrosion and precipitation. In: Pedley, H. M. & Rogerson, M. (eds), *Tufas and Speleothems: Unravelling the Microbial and Physical Controls. Geological Society Special Publications*, 336: 7–30.

Jones, B. & Kahle, Ch., 1993. Morphology, relationship, and origin of fiber and dendrite calcite crystals. *Journal of Sedimentary Petrology*, 63: 1018–1031.

Jones, B. & Ng, K.-C., 1988. The structure and diagenesis of rhizoliths from Cayman Brac, British West Indies. *Journal of Sedimentary Petrology*, 58: 457–467.

Jones, B. & Peng, X., 2012. Amorphous calcium carbonate associated with biofilms in hot spring deposits. *Sedimentary Geology*, 269–270: 58–68.

Julia, R., 1983. Travertines. In: Scholle, P. A., Bebout, D. G. & Moore, C. H. (eds), *Carbonate Depositional Environments. American Association of Petroleum Geologists Memoire*, 33: 64–72.

Kabanov, P. B., Alekseeva, T. V., Alekseeva, V. A., Alekseev, A. O. & Gubin, S. V., 2010. Paleosols in Late Moscovian (Carboniferous) marine carbonates of the East European Craton revealing 'great calcimagnesian plain' paleolandscapes. *Journal of Sedimentary Research*, 80: 195–215.

Kostrakiewicz, L., 1982. Klimat. In: Zarzycki, K. (ed.), *Przyroda Pienin w obliczu zmian*. Państwowe Wydawnictwo Naukowe, Warszawa, pp. 53–69. [In Polish].

Kowalinski, S., Pons, J. L. & Slager, S., 1972. Micromorphological comparison of three soils derived from loess in different climatic regions. *Geoderma*, 7: 141–158.

Krąpiec, M. & Walanus, A., 2011. Application of the triple-photomultiplier liquid spectrometer Hidex 300SL in radiocarbon dating. *Radiocarbon*, 53: 543–550.

Lacelle, D., Pellerin, A., Clark, J. D., Lauriol, B. & Fortin, D., 2009. (Micro)morphological, inorganic-organic isotope geochemistry and microbial populations in endostromatolites (cf. fissure calcretes), Haughton impact structure, Devon Island, Canada: The influence of geochemical pathways on the preservation of isotope biomarkers. *Earth and Planetary Science Letters*, 281: 202–214.

Lauriol, B. & Clark, I., 1999. Fissure calcretes in the arctic: A paleohydrologic indicator. *Applied Geochemistry*, 14: 775–785.

Loisy, C., Verrecchia, E. P. & Dufour, P., 1999. Microbial origin for pedogenic micrite associated with carbonate paleosol (Champagne, France). *Sedimentary Geology*, 126: 193–204.

Łącka, B., Łanczont, M. & Madeyska, T., 2009. Oxygen and carbon stable isotope composition of authigenic carbonates in loess sequences from the Carpathian margin and Podolia, as a palaeoclimatic record. *Quaternary International*, 198: 136–151.

Milliere, L., Hasinger, O., Bindschedler, S., Cailleau, G., Spangenberg, J. E., Verrecchia, E. P., 2011a. Stable carbon and oxygen isotope signatures of pedogenic needle fibre calcite. *Geoderma*, 161: 74–87.

Millière, L., Spangenberg, J. E., Bindschedler, S., Cailleau, G. & Verrecchia, E. P., 2011b. Reliability of stable carbon and oxygen isotope compositions of pedogenic needle fibre calcite as environmental indicators: examples from Western Europe. *Isotopes in Environmental and Health Studies*, 47: 341–358.

Morozewicz, J., 1907. Przyczynki do znajomości węglanu wapniowego. I. O lublinicie nowej odmianie spatu wapniowego. *Kosmos*, 32: 487–492. [In Polish].

Morozewicz, J., 1911. Ueber Lublinit, eine neue Vartietät des Kalkspates (Berichtigung.). *Centralblatt für Minerologie, Geologie und Paläontologie*, 1911: 229–231.

Northup, D. E. & Lavoie, K. H., 2001. Geomicrobiology of caves: A review. *Geomicrobiology Journal*, 18: 199–222.

O'Neil, J. R., Clayton, R. N. & Mayeda, T. K. 1969. Oxygen isotope fractionation in divalent metal carbonates. *Journal of Chemical Physics*, 51: 5547–5558.

Olszta, M. J., Gajjeraman, S., Kaufman, M. & Gower, L. B., 2004. Nanofibrous calcite synthesized via a solution–precursor–solid mechanism. *Chemistry of Materials*, 16: 2355–2362.

Onac, B. P., 1995. Minealogical data concerning moonmilk speleothems in few caves from northern Norway. *Acta Carsologica*, 24: 429–437.

Owliaie, H. R., 2013. Micromorphology of pedogenic carbonate features in soils of Kohgilouye, southwestern Iran. *Journal of Agricultural Science and Technology*, 14: 225–239.

Pazdur, A., Pazdur, M. F. & Szulc, J., 1988. Radiocarbon dating of Holocene calcareous tufa in southern Poland. *Radiocarbon*, 30, 133–152.

Pentecost, A., 2005. *Travertine*. Springer, Berlin, 445 pp.

Phillips, S. E. & Self, P. G., 1987. Morphology, crystallography and origin of needle-fibre calcite in Quaternary pedogenic calcretes of South Australia. *Australian Journal of Soil Research*, 25: 429–444.

Rajchel, L., Zuber, A., Duliński, M. & Rajchel. J., 2005. Isotope and chemical composition and water ages of sulphide springs in the Polish Carpathians. *Współczesne Problemy Hydrogeologii*, 12: 583–588. [In Polish, English summary].

Reimer, P. J., Bard, E., Bayliss, A., Beck, J. W., Blackwell, P. G., Ramsey, C. B., Buck, C. E., Cheng, H., Edwards, R. L., Friedrich, M., Grootes, P. M., Guilderson, T. P., Haflidison, H., Hajdas, I., Hatté, C., Heaton, T., Hoffmann, D. L., Hogg, A., Hughen, K. A., Kaiser, K., Kromer, B., Manning, S. W., Niu, M., Reimer, R., Richards, D.,A., Scott, E. M., Southon, J. R., Staff, R. A., Turney, C. & Plicht, J., 2013. IntCal13 AND Marine13 radiocarbon age calibration curves 0–50,000 years cal BP. *Radiocarbon*, 55: 1869–1887.

Richter, D. K., Immenhauser, A. & Neuser, R. D., 2008. Electron backscatter diffraction documents randomly oriented *c*-axes in moonmilk calcite fibres: evidence for biologically induced precipitation. *Sedimentology*, 55: 487–497.

Rodriguez-Blanco, J. D., Shaw, S. & Benning, L. G., 2011. The kinetics and mechanisms of amorphous calcium carbonate (ACC) crystallization to calcite, *via* vaterite. *Nanoscale*, 3: 265–271.

Rossinsky, V, Jr., Wanless, H. R. & Swart, P. K., 1992. Penetrative calcretes and their stratigraphic implications. *Geology*, 20: 331–334.

Rozanski, K. & Dulinski, M., 1988. A reconnaissance isotope study of waters in the karst of the Western Tatra Mountains. *Catena*, 15: 289–301.

Sherman, C. E., Fletcher, C. H. & Rubin, K. H., 1999. Marine and meteoric diagenesis of Pleistocene carbonates from a nearshore submarine terrace, Oahu, Hawaii. *Journal of Sedimentary Research*, 69: 1083–1097.

Stoops, G. J., 1976. On the nature of "lublinite" from Hollanta

(Turkey). *American Mineralogist*, 61: 172.

Strong, G. E., Giles, J. R. A. & Wright, V. P., 1992. A Holocene calcrete from North Yorkshire, England: implications for interpreting palaeoclimates using calcretes. *Sedimentology*, 39: 333–347.

Supko, P. R., 1973. "Whisker" crystal cement in a Bahamian rock. In; Bricker, O.P. (ed.), *Carbonate Cements. John Hopkins University Studies in Geology*, 19: 143–146.

Szulc, J. & Smyk, B., 1994. Bacterially controlled calcification of freshwater *Schizotrix*-stromatolites: an example from the Pieniny Mts., Southern Poland. In: Bertrand-Sarfati, J. & Monty, C. (eds), *Phanerozoic Stromatolites II*. Kluwer, Dordrecht, pp. 31–51.

Thugutt, S, J., 1929. Sur la nature de la lublinite et sa solubilité dans l'eau distillée. *Archiwum Mineralogiczne*, 5: 97–104. [In Polish, French summary].

Verrecchia, E. P., 1990. Lithodiagenetic implications of the calcium oxalate-carbonate biogeochemical cycle in semi arid calcretes, Nazareth, Israel. *Geomicrobiology Journal*, 8: 89–101.

Verrecchia, E. P. & Verrecchia, K. E., 1994. Needle-fiber calcite: A critical review and a proposed classification. *Journal of Sedimentary Research*, A64: 650–664.

Ward, W. C., 1973. Influence of climate on the early diagenesis of carbonate eolianites. *Geology*, 1: 171–174.

Wright, V. P., 1984. The significance of needle-fibre calcite in Lower Carboniferous palaeosol. *Geological Journal*, 19: 831–838.

Wright, V. P., 1986. The role of fungal biomineralization in the formation of early Carboniferous soil fabrics. *Sedimentology*, 33: 831–838.

Wright, V. P., 2007. Calcrete. In: Nash, D. J. & McLaren, S. J. (eds), *Geochemical Sediments and Landscapes*. Blackwell, Malden, pp. 10–45.

Wright, V. P., Platt, N. H., Mariott, S. B. & Beck, V. H., 1995. A classification of rhizogenic (root-formed) calcretes, with examples from the Upper Jurassic-Lower Cretaceous of Spain and Upper Cretaceous of southern France. *Sedimentary Geology*, 110: 143–158.

Xu, X., Han, J. T. & Cho, K., 2005. Deposition of amorphous calcium carbonate hemispheres on substrates. *Langmuir*, 21: 4801–4804.

Xu, X.-R., Cai, A.-H., Liu, R., Pan, H.-H., Tang, R.-K. & Cho, K., 2008. The roles of water and polyelectrolytes in the chase transformation of amorphous calcium carbonate. *Journal of Crystal Growth*, 310: 3779–3787.

Zhou, J. & Chafetz, H. S., 2009. Biogenic caliches in Texas: The role of organisms and effect of climate. *Sedimentary Geology*. 222: 207–225.